Antiferromagnetism. The Triangular Ising Net

G. H. WANNIER
Bell Telephone Laboratories, Murray Hill, New Jersey
(Received February 11, 1950)

In this paper the statistical mechanics of a two-dimensionally infinite set of Ising spins is worked out for the case in which they form either a triangular or a honeycomb arrangement. Results for the honeycomb and the ferromagnetic triangular net differ little from the published ones for the square net (Curie point with logarithmically infinite specific heat). The triangular net with antiferromagnetic interaction is a sample case of antiferromagnetism in a non-fitting lattice. The binding energy comes out to be only one-third of what it is in the ferromagnetic case. The entropy at absolute zero is finite; it equals

$$S(0)=R\frac{2}{\pi}\int_0^{\pi/3}\ln(2\cos\omega)d\omega=0.3383R.$$

The system is disordered at all temperatures and possesses no Curie point.

I. INTRODUCTION

THANKS to the work of Kaufman and Onsager[1–3] we are now in possession of a method of solving exactly a certain number of cooperative problems in physics. We can obtain the thermal properties and some order-parameters for a two-dimensional periodic structure whose members are "spins" capable of existing in two states; these spins interact with their nearest neighbors only, according to the mode put forward by Ising.[4] In addition to the general theory, the papers quoted contain also its application to the rectangular Ising net which is shown in Fig. 1. The main feature of their results is the temperature singularity. The singularity is mainly known at this time through its manifestation in the specific heat curve. For a complete study of this "Curie point" transition one would like to know also the magnetic properties. These quantities are not available in the literature at this time although the spontaneous magnetization has been calculated.[5]

In the original calculations the Ising model was thought of as ferromagnetic. Within recent years, however, antiferromagnetism has received considerable attention, and one might wish to think of the model in terms of this new application. The salient features of antiferromagnetism are described in an article of Bizette.[6] The specific heat resembles that of ferromagnetic materials; the susceptibility curves resemble the specific heat curves somewhat, having a pronounced maximum at the Curie point. Both these features can be accounted for qualitatively on the basis of nearest neighbor interaction. The specific heat calculation of Onsager[1] actually does not distinguish at all between ferromagnetism and antiferromagnetism, owing to the well-known symmetry property which applies to all lattices having α- and β-sites with all α-sites surrounded by β-sites and vice versa.

A closer study of antiferromagnetism removes to a great extent this superficial similarity. It may be seen from the work of Hulthén[7] that the difference between the quantum and Ising interactions is much more drastic in the antiferromagnetic than the ferromagnetic case. Specifically, a linear chain of quantum spins whose interaction is $J\Sigma\boldsymbol{\sigma}_i\cdot\boldsymbol{\sigma}_{i+1}$ has a lowest energy which is 1.775 times that of a corresponding set of Ising spins. This situation is in contrast to the ferromagnetic case and by itself removes any hope of a simple analogy. In addition, the antiferromagnetic materials MnO, MnS, MnTe, FeO crystallize in the NaCl structure; this gives the paramagnetic metal ions a face-centered cubic arrangement. Such an arrangement of sites does not divide into α- and β-sites in the manner described above. In consequence, even for an Ising antiferromagnet the thermal properties are not trivally related to some "equivalent" ferromagnetic arrangement.

This paper is one in a series of related studies on these non-trivial aspects of antiferromagnetism. We will derive in it the properties of an antiferromagnetic triangular Ising net (Fig. 2). This arrangement is a two-dimensional analog of the face-centered cubic structure, in that it is also a lattice into which antiferromagnetism does not fit. The Kaufman-Onsager calculation can be carried out for it and full results obtained. We shall

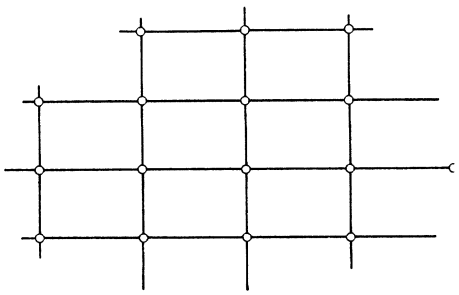

FIG. 1. Rectangular Ising net. The circles indicate the location of the spins and the straight lines the interactions.

[1] L. Onsager, Phys. Rev. **65**, 117 (1944).
[2] Kaufman, Phys. Rev. **76**, 1232 (1949).
[3] B. Kaufman and L. Onsager, Phys. Rev. **76**, 1244 (1949).
[4] E. Ising, Zeits. f. Physik **31**, 253 (1925).
[5] B. Kaufman (private communication).
[6] H. Bizette, thesis, Paris, Masson et Cie, pp. 62–96.
[7] L. Hulthén, Arkiv f. Mat. Astr. o. Fys. **26A**, No. 11 (1938).

find that the lowest energy state of the model is disordered and actually possesses a finite entropy; there is no discontinuity in the specific heat and probably no maximum in the susceptibility. Results for the ferromagnetic triangular net and the honeycomb net will be obtained as a by-product of the work; they do not differ essentially from the results obtained for the square net.[1-3]

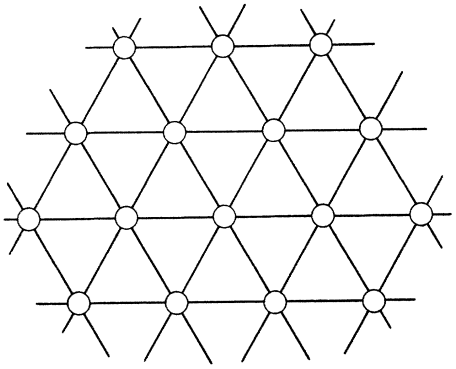

FIG. 2. Triangular Ising net. No perfectly regular antiferromagnetic arrangement can be fitted into this structure.

II. QUALITATIVE DISCUSSION

It is convenient to discuss by simpler methods two salient features of the triangular net; namely, the ferromagnetic Curie point and the antiferromagnetic zero-point entropy.

The derivation which locates the Curie point and establishes the symmetry property about that point may be found elsewhere in the literature.[8] We will not return to this derivation, but make use of the results.

The calculations involve one parameter L only, which is defined as

$$L=J/(2kT), \tag{1}$$

where J is the coupling energy (energy required to turn over one pair of spins from the parallel to the antiparallel position), k is Boltzmann's constant, and T is the temperature. It is shown in reference 8 how the partition function for any two-dimensional net is linked with the partition function for the "dual" which is constructed from the first by replacing all areas by points and vice versa. The dual for the triangular net is the honeycomb; their mutual relationship is illustrated in Fig. 3. This dual relationship involves a "dual" temperature L^*. It is shown in reference 8 that the relation between L and L^* is

$$\sinh 2L \sinh 2L^*=1, \tag{2a}$$

or

$$\tanh^2 2L+\tanh^2 2L^*=1, \tag{2b}$$

or

$$\cosh 2L \tanh 2L^*=\cosh 2L^* \tanh 2L=1. \tag{2c}$$

The dual relationship for the partition functions is given in reference 8, Eq. (23). For infinite systems we may suppress a negligible factor $\sinh 2L$ and write it in the form

$$f(L)/(2\sinh 2L)^{N/2}=f^*(L^*)/(2\sinh 2L^*)^{N^*/2}. \tag{3}$$

Although this dual relation is a reversible one, we shall use it in the following in a one-sided way and preferably associate the star with the honeycomb.

It is possible to return from $f^*(L^*)$ to f by a second algebraically independent transformation, the so-called star-triangle transformation.[8] The transformation is illustrated in Fig. 4. In the state sum, f^*, the summation is carried out over all spins, μ. In executing this sum, one can, however, divide them into two classes which are marked, respectively, by full and open circles in Fig. 4. The sum over the open circles is carried out first; this is relatively simple because the summation over μ_0 in Fig. 4 involves only the three spins μ_1, μ_2, and μ_3.

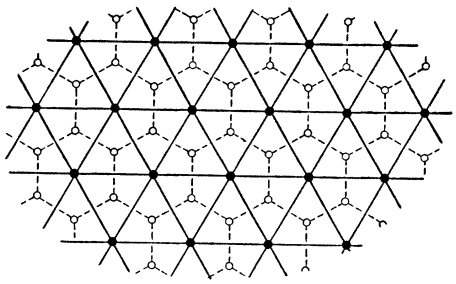

FIG. 3. Dual relationship between the triangular and the honeycomb net. Areas replace corners in a reciprocal fashion, sides replace sides.

The result of the summation can be expressed by a fictitious interaction J^+ between μ_1, μ_2, and μ_3 which is shown in heavy dotted outline. These dotted interactions, when continued throughout the lattice produce again a triangular net, but with a new interaction J^+. Apart from certain factors, the partition function for the triangle net at the "temperature" L is thus equivalent to the same partition function at the "temperature" L^+ where L^+ is derived from J^+ by Eq. (1). The relation between L and L^+ is found to be[8] expressible in the forms

$$[\exp(4L)-1][\exp(4L^+)-1]=4, \tag{4a}$$

$$(\coth 2L-1)(\coth 2L^+-1)=1, \tag{4b}$$

$$\tanh 2L+\tanh 2L^+=1, \tag{4c}$$

and the symmetry relationship for f reads

$$f(L)/(2\sinh 2L)^{N/2}=f(L^+)/(2\sinh 2L^+)^{N/2}. \tag{5}$$

We shall refer to the temperature defined by (4) and (5) as the "inverted" temperature and to the process as temperature inversion. The dual temperature is thus the "inverted" temperature for the square net.

It may be noted that relationships (3) and (5) completely specify the temperature inversion for the honey-

[8] G. H. Wannier, Rev. Mod. Phys. **17**, 50 (1945), Part IV.

comb. We find that

$$f^*(L^*)/(2\sinh 2L^*)^{N^*/2}=f^*(L^{*+})/(2\sinh 2L^{*+})^{N^*/2}. \quad (6)$$

The relation between L^* and L^{*+} follows from (2c) and (4) as

$$\sinh L^* \sinh L^{*+}=\tfrac{1}{2}, \quad (7a)$$

or

$$\operatorname{sech} 2L^*+\operatorname{sech} 2L^{*+}=1. \quad (7b)$$

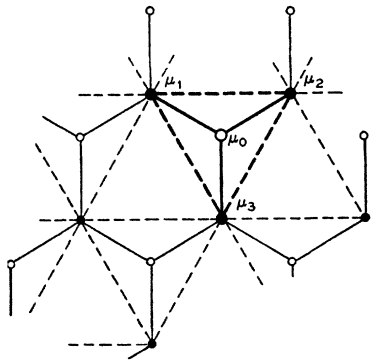

FIG. 4. Star-triangular transformation: Removal by summation of the open-circled spins from the honeycomb state sum (full lines) leaves a triangular net (dotted lines).

It is curious that the quantity entering into (3) is also the one entering into (5) and (6). At this time, this is not obvious from any previous reasoning.

The relationships (2), (4), and (7) locate the Curie point of the material as the point at which the temperature equals its inverse.

From the partition function, f, the internal energies are obtained by differentation

$$U=-\tfrac{1}{2}Jd(\ln f)/dL. \quad (8)$$

Thus each of the relations (3), (5), and (6) has a corrollary involving the energies U. We shall restrict outselves to (3) which yields

$$\frac{U(L)}{-\frac{1}{2}J\coth 2L}+\frac{U^*(L^*)}{-\frac{1}{2}J\coth 2L^*}=N+N^*=S, \quad (9)$$

where S is the number of sides of either one of the dual nets.

The second part of this qualitative discussion will be concerned with the antiferromagnetic triangular net.

It was mentioned that the thermal properties of the rectangular and honeycomb net are independent of the sign of the interaction J; this symmetry is also apparent in the relations (2) and (7). For the triangular net, however, we must expect entirely different results in the two cases.

The fact that antiferromagnetism does not fit into the triangular pattern modifies particularly the low temperature behavior because of a different type of ground state. The energy of this state is quite easily perceived to be only one-third of the corresponding ferromagnetic value. We prove this in two steps: first, we show that it cannot possibly be lower; second, we actually construct states of this energy.[9] For the first point we decompose the net into triangles as shown in Fig. 5. Each triangle contains three interactions, and the best we can achieve within each is to have two spins of one sign and one of the other. Thus the final arrangement contains at least one-third of the wrong interactions.

There are actually states in which the number of wrong interactions is just one-third which have therefore the energy minimum

$$U(0)=-\tfrac{1}{6}SJ=-\tfrac{1}{2}NJ. \quad (10)$$

An example of such an arrangement is shown in Fig. 6. It consists of rows of positive spins alternating with rows of negative spins. It is not likely to be ever realized because there are arrangements of much higher weight.

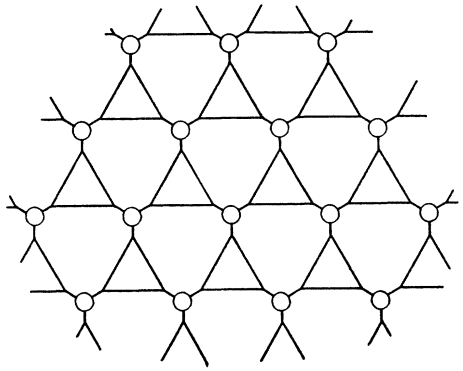

FIG. 5. Decomposition of the triangular net into individual triangles. Each interaction forms part of one and only one triangle. At least two neighbors must be equal in each triangle.

Figure 7 shows one which consists of rows of alternate spins. Each row may be laid independently; i.e., we may commit a large number of "stacking errors" and still stay in the ground state. The entropy of the arrangement is still zero because the weight is proportional to $N^{\frac{1}{2}}$ only. In Fig. 8, on the other hand, we have an arrangement of finite entropy.[10] We see that in this arrangement the correct energy is obtained by an unbalance; around a (+) spin the ratio of right and wrong interactions is 6:0, while for the more numeous (−) spins it is 3:3. From this latter ratio it follows that we can reverse any one of the negative spins without changing the energy. We may even perform this operation independently for each one of the encircled negative spins and thus gain a weight of $2^{N/3}$. This is not yet the full weight because there is a large amount of contingent freedom. Since the encircled spins can be varied independently, it will occur quite often that three encircled spins forming a triangle have equal sign. In the overwhelming majority of cases (by the arguments of fluctuation theory) each of the arrangements

[9] The following proof is due to W. Shockley.

[10] The following considerations are due to P. W. Anderson.

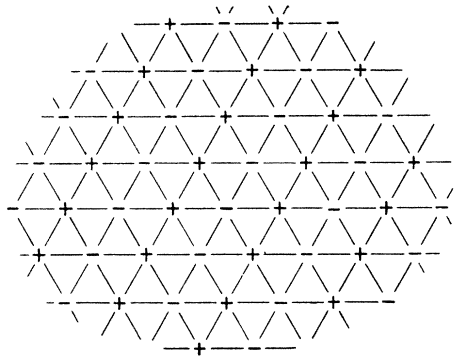

FIG. 6. A simple arrangement of minimum energy: Rows of positive spins placed in alteration with rows of negative spins.

of Fig. 9 will prevail at least at one out of eight positions. It now happens for the center spin of this tripod that its interactions are in the ratio 3:3. Hence it may be reversed also and there are another $(N/24)+(N/24)$ free spins added to the original number of $N/3$. The weight of the ground state thus is pushed to $2^{5N/12}$; it is clear that it may be pushed up further by consideration of more involved contingencies. We thus have for the zero-point entropy

$$S(0)>(5/12)R\ln 2=0.288811R. \tag{11}$$

The exact value of this entropy will be derived later (Eq. (37)).

Long-range order is incompatible with a ground state of this type. As an example, there is shown in Fig. 10, an arrangement in which two ordered sections of the type shown in Fig. 8 adjoin. Long-range order in each ordered section is different and a transition region results. This region has, however, the same low energy as do the ordered regions themselves. We conclude therefore that long-range order offers no energy advantage for this structure.

It has been mentioned earlier that we are not able, at this time, to compute the paramagnetic susceptibility. We can, however, draw qualitative conclusions easily. The situation exemplified by Fig. 10 clearly implies an infinite susceptibility at absolute zero. After that, the susceptibility must drop and there is no physical reason to expect that magnetization will ever become easier as the temperature rises. Thus we would expect a paramagnetic sort of a curve which is at variance with experimental observations.[6]

III. CALCULATION OF THE THERMAL PROPERTIES

We shall, in this section, supplement the considerations of Section II by calculating explicitly the thermal properties of the triangular net; these can be obtained by applying the methods of Kaufman and Onsager.[1–3] The reader is assumed to be familiar with this earlier work and we shall only note the necessary modifications.

The honeycomb may be deformed topologically to take the appearance of a "brick" net (Fig. 11). This rectangular arrangement differs from the one studied in reference 1 only in that certain interactions are missing. This means some minor modification in the basic operations.

We shall assume that the brick net is being built up sideways rather than upward. No interaction is then missing in the direction of the build-up and the operator V_1 can be taken over unaltered from reference 1, Eq. (21) as

$$V_1=(2\sinh 2L^*)^{n/2}e^{LB}. \tag{12}$$

The reversal of the dual star is in accordance with the convention adopted earlier. In place of the operator V_2 defined in reference 1, Eq. (28), we have two operators V_3 and V_4 which alternate. They are, respectively,

$$V_3=\exp H^*(s_1s_2+s_3s_4+\cdots), \tag{13}$$

$$V_4=\exp H^*(s_ns_1+s_2s_3+\cdots). \tag{14}$$

The partition function is obtained by using these

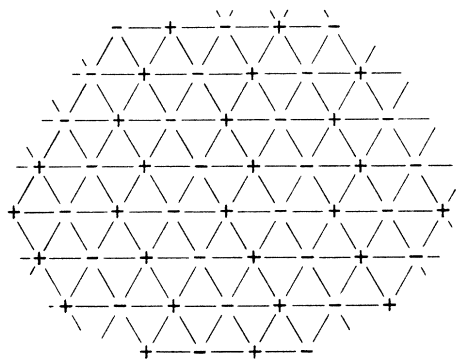

FIG. 7. An arrangement of minimum energy having medium-high weight: Rows of alternating spins stacked at random.

operators in the arrangement

$$\cdots V_1V_3V_1V_4V_1V_3V_1V_4V_1\cdots.$$

Two rows of spins will have to be laid down before the cycle repeats. Consequently, Eq. (29) of reference 1 is replaced by

$$\lambda\psi=(V_3V_1V_4V_1)\psi. \tag{15}$$

Among the various steps which follow (15), the passage to operators P_i, Q_i defined in reference 2 requires some discussion. This necessary transition introduces unsymmetric end terms, such as the one in reference 2, Eq. (14). The author feels that it is not generally worth while to pay too much attention to such terms. Bulk properties and even short-range order should be unaffected by a modification of the "seam." Long-range order is probably affected because such a modification of operators may remove the degeneracy. It is known that degeneracy is essential for the study of long-range order.[11] Apart from such special require-

[11] J. Ashkin and W. E. Lamb, Phys. Rev. **64**, 159 (1943).

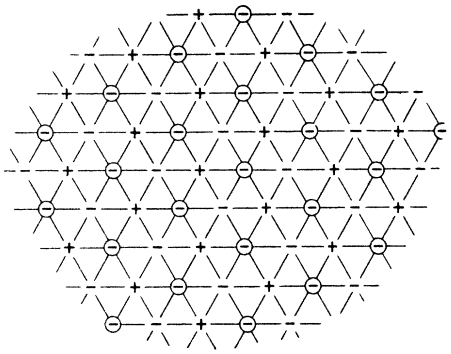

FIG. 8. An arrangement of minimum energy having finite entropy: Two sublattices have spins of fixed sign, but in the third, each sign individually may be picked at random.

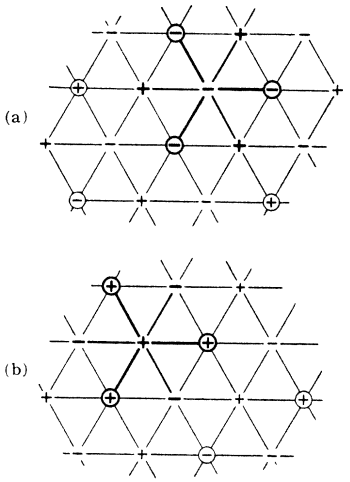

FIG. 9. Two arrangements (a, b) of contingent freedom. If three neighboring ringed spins of Fig. 8 happen to have equal sign, their center may be chosen at random. Such considerations make the entropy larger than $\frac{1}{3}R\ln 2$.

ments we may disregard this refinement and consider Eq. (41) of reference 2 as the matrix of the rectangular Ising problem (apart from a factor dropped in passing from Eqs. (4) to (8) of reference 2). Its analog for the brick lattice is obvious; it contains three rather than two types of factors, each of which represents a set of commuting plane rotations. We write the rotation represented by V_1 in the form

$$\begin{pmatrix} \cosh 2L & & & & & & & -i\sinh 2L \\ & \cosh 2L & i\sinh 2L & & & & & \\ & -i\sinh 2L & \cosh 2L & & & & & \\ & & & \cosh 2L & i\sinh 2L & & & \\ & & & -i\sinh 2L & \cosh 2L & & & \\ & & & & & \cdot & & \\ & & & & & & \cdot & \\ & & & & & & & \cdot \\ i\sinh 2L & & & & & & & \cosh 2L \end{pmatrix}. \tag{16}$$

Similarly V_3 represents the matrix

$$\begin{pmatrix} \cosh 2L^* & i\sinh 2L^* & & & & & & \\ -i\sinh 2L^* & \cosh 2L^* & & & & & & \\ & & 1 & & & & & \\ & & & 1 & & & & \\ & & & & \cosh 2L^* & i\sinh 2L^* & & \\ & & & & -i\sinh 2L^* & \cosh 2L^* & & \\ & & & & & & \cdot & \\ & & & & & & & \cdot \\ & & & & & & & \cdot \end{pmatrix}. \tag{17}$$

Finally, V_4 represents the matrix

$$\begin{pmatrix} 1 & & & & & & & \\ & 1 & & & & & & \\ & & \cosh 2L^* & i\sinh 2L^* & & & & \\ & & -i\sinh 2L^* & \cosh 2L^* & & & & \\ & & & & 1 & & & \\ & & & & & 1 & & \\ & & & & & & \cosh 2L^* & \\ & & & & & & & \cdot \\ & & & & & & & \cdot \\ & & & & & & & \cdot \end{pmatrix}. \tag{18}$$

The analysis following Eq. (43) of reference 2 applies to the present case except that $f=4$. The resultant matrix

has the same form as their Eq. (50) with

$$a=\begin{pmatrix} \cosh 2L^*\,(\cosh^2 2L+\sinh^2 2L\cosh 2L^*) & i\sinh 2L^*\,(\cosh^2 2L+\sinh^2 2L\cosh 2L^*) & -\cosh 2L\sinh 2L\,(1+\cosh 2L^*)\sinh 2L^* & -i\cosh 2L\sinh 2L\sinh^2 2L^* \\ -i\sinh 2L^*\,(\cosh^2 2L+\sinh^2 2L\cosh 2L^*) & \cosh 2L^*\,(\cosh^2 2L+\sinh^2 2L\cosh 2L^*) & i\cosh 2L\sinh 2L\,(1+\cosh 2L^*)\cosh 2L^* & -\cosh 2L\sinh 2L\cosh 2L^*\sinh 2L^* \\ 0 & -i\cosh 2L\sinh 2L\,(1+\cosh 2L^*) & \cosh^2 2L\cosh 2L^*+\sinh^2 2L & i\cosh^2 2L\sinh 2L^* \\ 0 & -\cosh 2L\sinh 2L\sinh 2L^* & -i\cosh^2 2L\sinh 2L^* & \cosh^2 2L\cosh 2L^*+\sinh^2 2L \end{pmatrix} \tag{19}$$

$$b=\begin{pmatrix} \sinh^2 2L\sinh^2 2L^* & 0 & 0 & 0 \\ -i\sinh^2 2L\cosh 2L^*\sinh 2L^* & 0 & 0 & 0 \\ -\cosh 2L\sinh 2L\sinh 2L^* & 0 & 0 & 0 \\ i\cosh 2L\sinh 2L\,(1+\cosh 2L^*) & 0 & 0 & 0 \end{pmatrix} \tag{20}$$

$$c=\begin{pmatrix} 0 & i\sinh^2 2L\cosh 2L^*\sinh 2L^* & \cosh 2L\sinh 2L\cosh 2L^*\sinh 2L^* & -i\cosh 2L\sinh 2L\,(\cosh 2L^*+1)\cosh 2L^* \\ 0 & \sinh^2 2L\sinh^2 2L^* & i\cosh 2L\sinh 2L\sinh^2 2L^* & -\cosh 2L\sinh 2L\,(\cosh 2L^*+1)\sinh 2L^* \\ 0 & 0 & 0 & 0 \\ 0 & 0 & 0 & 0 \end{pmatrix} \tag{21}$$

The secular equation of this matrix has the form

$$x^4-Ax^3+Bx^2-Ax+1=0. \tag{22}$$

The roots are therefore pairs of reciprocals and the substitution

$$x=e^{\gamma} \tag{23}$$

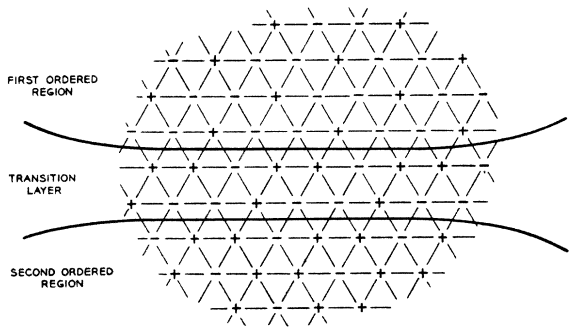

FIG. 10. Two adjoining regions having different types of long-range order. The energy of the transition layer may be made just as low as that of the ordered regions.

yields a quadratic equation in $\cosh\gamma$. This equation is

$$\cosh^2\gamma-(\kappa^{-1}-1+\cos\omega)\cosh\gamma+\tfrac{1}{4}\kappa^{-2}-\kappa^{-1}-\cos\omega=0, \tag{24}$$

where

$$\epsilon^2+\epsilon^{-2}=2\cos\omega \tag{25}$$

and

$$\kappa=(e^{4L}-1)/(e^{4L}+1)^2. \tag{26}$$

κ is a symmetric parameter similar to that defined in reference 1, Eq. (114). It is zero for high or low temperatures and reaches a maximum of $\frac{1}{8}$ at the Curie point; for antiferromagnetic interactions it is negative. In view of this symmetry, the roots of (24) are invariant with respect to temperature inversion and the only asymmetric factor entering into the partition function is the scalar factor evident in (12). We thus get the analog of reference 2, Eq. (71), as

$$f^*(L^*)=(2\sinh 2L^*)^n\Pi^{\frac{1}{2}n}{}_{m=1}\exp[\tfrac{1}{2}\gamma_1{}^{(m)}+\tfrac{1}{2}\gamma_2{}^{(m)}], \tag{27}$$

where γ_1 and γ_2 are the two roots of (24) with $\omega=\omega^{(m)}$ and

$$\omega^{(m)}=4\pi m/n. \tag{28}$$

The expression obtained is for two rows of n spins in the arrangement of Fig. 11; i.e., for $2n$ spins in the honeycomb. Thus $N^*=2n$, and the factor in (27) is just the asymmetric factor to be expected from (3). An inspection of Fig. 3 shows that

$$N=\tfrac{1}{2}N^*=n.$$

The expression (27) becomes thus the partition function for n triangular spins; altering factors according to (3) we arrive thus at the partition function $\lambda(L)$ per spin of the triangular net as

$$\lambda^n=(2\sinh 2L)^{n/2}\Pi_{m=1}^{\frac{1}{2}n}\exp[\tfrac{1}{2}\gamma_1^{(m)}+\tfrac{1}{2}\gamma_2^{(m)}] \quad (29)$$

or, passing to the limit of infinite n and using Eq. (28), we find

$$\ln\lambda=\tfrac{1}{2}\ln(2\sinh 2L)+\frac{1}{8\pi}\int_0^{2\pi}[\gamma_1(\omega)+\gamma_2(\omega)]d\omega. \quad (30)$$

We use the solution of (24) in the form

$$\cosh\tfrac{1}{2}\gamma=\tfrac{1}{2}[\kappa^{-1}+\cos^2\tfrac{1}{2}\omega]^{\frac{1}{2}}\pm\tfrac{1}{2}\cos\tfrac{1}{2}\omega. \quad (31)$$

This gives

$$\ln\lambda=\frac{1}{2}\ln(2\sinh 2L)+\frac{1}{4\pi}\int_0^{2\pi}\operatorname{arc\,cosh}\left[\frac{1}{2}\left(\frac{1}{\kappa}+\cos^2\frac{\omega}{2}\right)^{\frac{1}{2}}+\frac{1}{2}\cos\frac{\omega}{2}\right]d\omega+\frac{1}{4\pi}\int_0^{2\pi}\operatorname{arc\,cosh}\left[\frac{1}{2}\left(\frac{1}{\kappa}+\cos^2\frac{\omega}{2}\right)^{\frac{1}{2}}-\frac{1}{2}\cos\frac{\omega}{2}\right]d\omega.$$

We apply the identity (107) of reference 1 to the integrals and observe that the sign of the cos term occurring there is immaterial; thus we get

$$\ln\lambda=\frac{1}{2}\ln(2\sinh 2L)+\frac{1}{8\pi^2}\int_0^{2\pi}\int_0^{2\pi}\ln\left[\left(\frac{1}{\kappa}+\cos^2\frac{\omega}{2}\right)^{\frac{1}{2}}+\cos\frac{\omega}{2}-2\cos\omega'\right]d\omega d\omega'+\frac{1}{8\pi^2}\int_0^{2\pi}\int_0^{2\pi}\ln\left[\left(\frac{1}{\kappa}+\cos^2\frac{\omega}{2}\right)^{\frac{1}{2}}-\cos\frac{\omega}{2}+2\cos\omega'\right]d\omega d\omega'.$$

Combining the integrals and using (26) we reduce this to the form

$$\ln\lambda=\ln(e^{3L}+e^{-L})+\frac{1}{8\pi^2}\int_0^{2\pi}\int_0^{2\pi}\ln[1+4\kappa\cos\omega\cos\omega'-4\kappa\cos^2\omega']d\omega d\omega'. \quad (32)$$

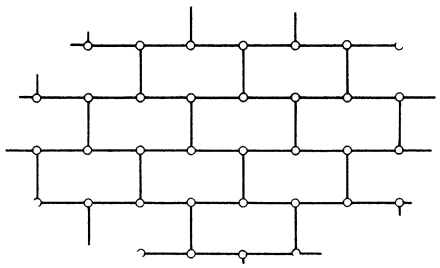

FIG. 11. The "brick" net. When all interactions are taken to be equal the net is equivalent to the "honeycomb" of Fig. 3. However, it suggests a way of applying the method of Kaufman and Onsager which is basically rectangular.

Employing the substitution

$$\omega'=\tfrac{1}{2}(\omega_1+\omega_2),\quad \omega=\tfrac{1}{2}(\omega_1-\omega_2),$$

we obtain

$$\ln\lambda=\ln(e^{3L}+e^{-L})+\frac{1}{8\pi^2}\int_0^{2\pi}\int_0^{2\pi}\ln[1-2\kappa+2\kappa\cos\omega_1+2\kappa\cos\omega_2+2\kappa\cos(\pi-\omega_1-\omega_2)]d\omega_1 d\omega_2. \quad (33)$$

The form (33) is of the type first suspected by Kac and Berlin.[12] The number of cos terms equals the number of linkages and the number of integrations equals the number of dimensions.

Applying formula (8) to Eq. (32), we find for the

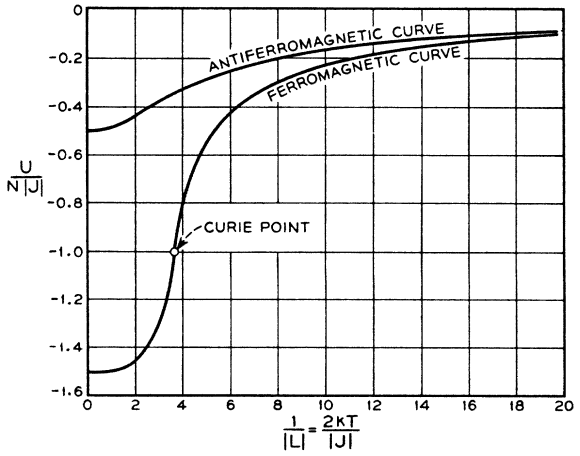

FIG. 12. Energy-*vs.*-temperature plot for the triangular Ising net. Ferromagnetic and antiferromagnetic coupling.

[12] M. Kac and T. Berlin (private communication).

energy U

$$\frac{U}{-\frac{1}{2}NJ}=\coth 2L-\frac{2e^{4L}(3-e^{4L})}{\pi(e^{4L}+1)^3\kappa}\cdot\int_{-1}^{+1}\frac{dx}{[(1-x^2)((1-2\kappa)^2-4\kappa x-4\kappa^2x^2)]^{\frac{1}{2}}}.$$

The integral is a complete elliptic integral of the first kind. Because of Landen's identity, its reduction to the standard integral $K(k)$ is not a complete determinate process. The most convenient reduction happens to differ from the one found in handbooks. It is

$$\int_\gamma^\beta\frac{dx}{[(\alpha-x)(\beta-x)(x-\gamma)(x-\delta)]^{\frac{1}{2}}}=2K\left\{\frac{[(\alpha-\gamma)(\beta-\delta)]^{\frac{1}{2}}-[(\alpha-\beta)(\gamma-\delta)]^{\frac{1}{2}}}{[(\alpha-\gamma)(\beta-\delta)]^{\frac{1}{2}}+[(\alpha-\beta)(\gamma-\delta)]^{\frac{1}{2}}}\right\}\Big/\{[(\alpha-\gamma)(\beta-\delta)]^{\frac{1}{2}}+[(\alpha-\beta)(\gamma-\delta)]^{\frac{1}{2}}\}.$$

This gives in our case

$$\frac{U}{-\frac{1}{2}NJ}=\frac{2}{1-\mu}\left\{1-\frac{\mu(3-\mu)}{1+|\mu|}\frac{(2/\pi)K(k)}{[1+\frac{1}{4}(1-|\mu|)^2]^{\frac{1}{2}}}\right\}\tag{34}$$

where

$$k=\frac{1-|\mu|}{1+|\mu|}\left\{\frac{1+\frac{1}{4}(1+|\mu|)^2}{1+\frac{1}{4}(1-|\mu|)^2}\right\}^{\frac{1}{2}},\tag{35}$$

and

$$\mu=1-2\tanh 2L.\tag{36}$$

The parameter μ defined here is a very convenient one with which to express the results. It is not itself invariant against temperature inversion, but its square is, as may be seen from (4c). When μ varies from -1 to $+3$ it covers both the ferromagnetic and antiferromagnetic range; this can be observed from the following juxtaposition

$\mu=-1$ ferromagnetic absolute zero, $U=-\frac{3}{2}NJ$,

$\mu=0$ ferromagnetic Curie point, $U=-NJ$,

$\mu=1$ {ferromagnetic / antiferromagnetic} high temperature, $U=0$,

$\mu=3$ antiferromagnetic absolute zero, $U=-\frac{1}{2}N|J|$.

Results for the honeycomb follow from the above by application of (2) and (9).

Curves which illustrate formula (34) are plotted in Fig. 12. The energy-*vs.*-temperature curve for the ferromagnetic triangular net is in all essentials identical with the one for the square lattice. The antiferromagnetic one is new. It shows no singular point. The value of U at the absolute zero is only one-third of the ferromagnetic value.

To obtain the entropy at absolute zero, we return to Eq. (32) and set $\kappa=-1$, $L\to-\infty$. We get

$$\ln\lambda\cong|L|+\frac{1}{8\pi^2}\int_0^{2\pi}\int_0^{2\pi}\ln[1-4\cos\omega\cos\omega'+4\cos^2\omega']d\omega d\omega'.$$

Remembering that

$$\lambda=e^{-U/RT}e^{+S/R},$$

we see that the first term just re-establishes the energy value (11):

$$-U(0)/RT=|L|=|J|/2kT.$$

The second term is therefore the entropy

$$S(0)=\frac{R}{8\pi^2}\int_0^{2\pi}\int_0^{2\pi}\ln[1-4\cos\omega\cos\omega'+4\cos^2\omega']d\omega d\omega'.$$

The integral over ω can be found in tables.[13] It equals

$$4\pi\ln 12\cos\omega'1[1-D(2\cos\omega')]$$

where D is the Dirichlet function, $D(x)=1$ if $|x|<1$, $D(x)=0$ if $|x|>1$. Thus we get for the zero-point entropy

$$S(0)=\frac{2R}{\pi}\int_0^{\pi/3}\ln(2\cos\omega')d\omega'.\tag{37a}$$

The integral must be computed by numerical methods. By elementary considerations we can get the alternate expression

$$\frac{S(0)}{R}=\frac{3}{\pi}\int_0^{\pi/6}\ln(2\cos\omega)d\omega.\tag{37b}$$

The small interval suggests a power series in ω. We get from it

$$\frac{S(0)}{R}=\frac{1}{2}\ln 2-\frac{1}{12}\left(\frac{\pi}{6}\right)^2-\frac{1}{120}\left(\frac{\pi}{6}\right)^4-\frac{1}{630}\left(\frac{\pi}{6}\right)^6-\frac{17}{45360}\left(\frac{\pi}{6}\right)^8-\cdots=0.338314\tag{37c}$$

in agreement with the inequality (11).

In conclusion the author wishes to express his thanks to his colleagues of the Bell Laboratories, particularly Dr. C. Kittel who first brought antiferromagnetism to his attention, and to Dr. P. W. Anderson and Dr. William Shockley who made the contributions mentioned in the text.

[13] Bierens de Hahn, *Nouvelles Tables d'Integrales Definies*, Table 330, integral 5.